Eur Food Res Technol (2008) 226:721–729
DOI 10.1007/s00217-007-0582-3

ORIGINAL PAPER

Fractal texture analysis of bread crumb digital images

Ursula Gonzales-Barron · Francis Butler

Received: 3 November 2006 / Revised: 16 January 2007 / Accepted: 22 January 2007 / Published online: 14 February 2007

Abstract A fractal texture analysis technique was applied to bread crumb digital images. Fractal dimensions obtained from several methods (fractional Brownian motion, frequency domain, relative differential box-counting, morphological fractal, mass fractal and random walks methods) were investigated in order to determine their capability to accurately describe the surface roughness of bread crumb images or the visual appearance of bread crumb in meaningful terms. A total of 500 bread crumb images of different porosity and grain quality were analysed. It was found that bread crumb appearance could be effectively quantified by the fractal dimension of its digital image. Correlations of fractal dimensions with mean cell area, standard deviation of cell area and void fraction were variable for the fractal methods. While the mass fractal method measured better crumb heterogeneity, other methods quantified coarseness, cell–cell wall ruggedness and cell wall tortuosity. A vector comprising fractal dimensions would objectively depict crumb grain and would allow comparisons between different bread crumb images.

Keywords Bread crumb · Grain · Fractal analysis · Texture · Fractal dimension

U. Gonzales-Barron (✉) · F. Butler
Biosystems Engineering, School of Agriculture,
Food Science and Veterinary Medicine,
University College Dublin, Earlsfort Terrace,
Dublin 2, Ireland
e-mail: ursula.gonzalesbarron@ucd.ie

Introduction

Like many other porous systems, bread is inherently irregular in structure and therefore it is not straightforward to quantify its physical structure and quality. Among other important factors, the quality of a white bread loaf is related to its crumb structure or grain. Close examination of different slices reveals considerable variation in the cell size even within a single sample [1]. Relatively large cells characterise what is called an ''open'' grain (coarse grain), and, conversely, small cells create a ''close'' grain. However, it is possible to have a nearly-uniform open grain, a uniformly close grain (uniform or homogeneous grain in both cases), or a combination of variously-sized cells (not uniform or heterogeneous grain). Pyler [2] stated that the crumb texture is greatly influenced by the cell structure of the crumb, with fine, thin-walled, uniformly sized cells producing a softer and more elastic texture than a coarse, open and thick-walled cell structure. In addition, the crumb colour is perceptibly influenced by the fineness and homogeneity of the crumb grain. The finer the grain, the brighter will be the crumb colour as perceived by the human eye.

Fractal analysis has been recently applied to the study of a wide class of physical phenomena ranging from atomization process; flocculation behaviour on fouling layer resistance during juice microfiltration to multi-peaks curves obtained on compression of expanded extruded rice [3–5]. Many foodstuffs like agglomerated particulates, flowering vegetables or porous products have complex geometry in which a large category of structural irregularities exist, and in certain foods such attributes may persist over wide levels of magnification [6]. Fractal techniques can be

particularly useful to characterise food morphology because the highly irregular structures of many food materials may elude precise quantification by conventional means. In this way, the apparent fractal dimension or ruggedness of particles such as instant coffee [7], sodium caseinate [8] and ice crystal particles in frozen food [9] have been characterised. Quevedo et al. [10] characterised surface roughness by fractal dimensions of several food materials including some fruits and vegetables, bread crust, bloomed chocolate and gelatinising starch granules. However, little work has been conducted on the investigation of suitable fractal methods to characterise the visual appearance of other cellular-structured foodstuffs such as bread. Using a squashing procedure to determine fractal dimension, Amaku et al. [11] reported that white Italian bread showed a possible fractal structure, characterised by the dimension 2.81 ± 0.06. Applying a box-counting method [12], Liu et al. [13] calculated the fractal dimension for number of cells in bread crumb (1.89 ± 0.07) and the fractal dimension for the cell wall area (2.41 ± 0.16) from digitised images. Interestingly, these fractal dimensions were found to be independent of the bread crumb density. The objectives of this research were: (1) to evaluate whether six selected fractal texture methods (fractional Brownian motion method, frequency domain method, relative differential box-counting method, morphological method, mass fractal method and random walks method) can be applied to characterise bread crumb grain from digital images, and (2) to investigate whether there is any correlation between fractal dimension with other widely-used crumb features extracted using a thresholding technique (mean cell area, standard deviation of cell area and void fraction).

Materials and methods

The fractal concept

Technically, Mandelbrot [14] defined a fractal as a set for which the Hausdorff–Besicovitch dimension strictly exceeds the topological dimension. A general definition of a fractal dimension is given by the power-law scaling equation:

$$M(\varepsilon) = n\varepsilon^{1-\mathrm{FD}},$$

where M is the property to be measured (perimeter, area, number of cells), ε is the scale used, n is a constant and FD is the fractal dimension which depends on the analysed dimension (2-D or 3-D). Fractals are characterised by the following three properties: they are self-similar; they are not described by mathematical formula but recurrent dependencies; and their dimension is not an integer. However, a real-world object cannot be expected to be self-similar at all magnifications or length scales like a mathematically constructed fractal object. This does not mean that a fractal dimension cannot be determined or that such a dimension is not useful. Instead, real objects can be inspected only over a limited range of length scales subject to physical or biological considerations. For instance, in the case of macroscopical digital images, the resolution becomes a limiting factor; and in the case of microscopical images, the microstructure will definitely not show any similarity to the macroscopical object's shape. Nonetheless, real objects that are self-similar over only a limited but pertinent range of length scales can be described in terms of their fractal dimension without causing conceptual concerns. The resulting fractal dimension, though, can be treated only as an apparent or natural fractal dimension, which may serve as an index of morphological roughness or tortuosity [6]. Thus, fractal functions represent a good model for describing the rough, crenulated and crumpled 3-D surfaces typical of natural objects [15].

Image acquisition

The image acquisition of bread slices took place on the same day of purchase. Forty white bread loaves of the same commercial brand were sliced transversely using an electric slicer to obtain 15 mm thick slices. They were scanned in colour on both sides using a flatbed scanner (HP ScanJet 5470c, Hewlett Packard Co., CA, USA) with 350 dpi of resolution and the following settings: highlight 190, shadows 40, and midtones 1 (scanning software HP Precisionscan Pro, Hewlett Packard Co.). The images were saved in TIFF format. The centre of each slice was cropped in a square of 520 × 520 pixels (1 pixel ~ 0.00527 mm^2) and converted to grey-level image (8 bits). A set of 500 images that presented a wide range of porosity, crumb coarseness and crumb heterogeneity was evaluated.

Features from image thresholding

The bread crumb images were binarised (converted from grey-level to black and white) using an automated fuzzy measure thresholding method [16, 17]. One-pixel and two-pixel objects were cleaned out by an opening operation (erosion and dilation) with a two-row two-column structuring element of ones and small void areas within pores were filled. The following crumb

features were obtained: (1) mean cell area in mm^2 (MCA), the average of all cells areas present in the crumb image, (2) standard deviation of cell areas in mm^2 (stCA), (3) void fraction (VF), the fraction of the total area corresponding to the cells in the cut surface bread crumb. The fuzzy method, the crumb features extracted and the fractal methods (shown below) were written and run in Matlab 6.12 (The MathWorks Inc., Natick, MA, USA). The fractional Brownian motion method, the frequency domain method and the relative differential box-counting method utilised grey-level images while the morphological method, the pore mass fractal method and the random walks method utilised images previously binarised by the fuzzy thresholding algorithm [16].

Methods to determine fractal dimensions (FD)

Fractional Brownian motion method (FBM)

This method is based on the average absolute difference of pixel intensities. Textures possessing the property of self-similarity can be analysed using statistically self-similar stochastic fractals. The fractional Brownian motion (a nonstationary stochastic process) is an example of a statistical fractal that can be described by the Hurst coefficient [18, 19]. However, because of its nonstationarity, it is difficult to estimate this parameter directly from an observation of the FBM. Therefore, the fractal dimension can be estimated from the fractional Brownian noise, which is the difference of successive points in the FBM.

For a particular intersample distance d, the average absolute intensity difference E is determined from all possible pixels pairs in four directions (horizontal, vertical, diagonal and antidiagonal). For a surface exhibiting FBM the intensity $I(x, y)$ of a pixel must satisfy [18].

$$E \propto d^H,$$

where

$$E = \frac{\sum_{x=0}^{M-1}\sum_{y=0}^{N-1}\sum_{u=0}^{M-1}\sum_{v=0}^{N-1}|I(u,v)-I(x,y)|}{P},$$
$$d = \sqrt{(u-x)^2+(v-y)^2}.$$

M and N are the dimensions of the region, and P is the number of pixel pairs in the region. H is called the Hurst coefficient, which is the slope of the least squares linear regression of the logarithmic plot of E versus d. The fractal dimension FBM_d is calculated by

$$\mathrm{FBM}_d = 3 - H.$$

Frequency domain method

In this method, the fast Fourier transforms (FFT) are taken in the horizontal and vertical directions. The average horizontal $D_\mathrm{h}(f)$ and vertical $D_\mathrm{v}(f)$ power spectrum of the surface is a function of the frequency f and satisfies

$$D_\mathrm{h}(f) \propto f^{2-\beta_\mathrm{h}},$$
$$D_\mathrm{v}(f) \propto f^{2-\beta_\mathrm{v}},$$

where

$$\beta_\mathrm{h} = 2H_\mathrm{h} + 2,$$
$$\beta_\mathrm{v} = 2H_\mathrm{v} + 2.$$

Thus, the horizontal and vertical Hurst coefficients are determined from the slope of the logarithmic plot of $D_\mathrm{h}(f)$ versus f and $D_\mathrm{v}(f)$ versus f, respectively. The fractal dimensions of the region in the horizontal and vertical directions are:

$$\mathrm{FFT}_\mathrm{h} = 3 - H_\mathrm{h},$$
$$\mathrm{FFT}_\mathrm{v} = 3 - H_\mathrm{v}.$$

The average value of the vertical and horizontal fractal dimensions FFT_d was considered.

Relative differential box-counting method (RDBC)

Although the box-counting is a very simple method, some research has been performed [20–22] in order to prevent two problems usually associated with the traditional computerised box-counting method: the border effect and the box sizes. In this work, the modifications made by Jin et al. [23] were considered. At a certain scale level ε, the image is partitioned into grids of size $\varepsilon \times \varepsilon$. Within a single grid $g_\varepsilon(i, j)$, let the maximum and minimum grey levels be $u_\varepsilon(i, j)$ and $b_\varepsilon(i, j)$, respectively. For digital images, R (resolution, 520 pixels), G (number of grey levels, 256) and ε are finite integers, so there are some partitions of size smaller than $\varepsilon \times \varepsilon$ at the image margins. In such cases, the grey levels outside the image region are zero. The difference in maximum and minimum grey-level per grid is

$$d_\varepsilon(i,j) = u_\varepsilon(i,j) - b_\varepsilon(i,j).$$

Taking contributions from all grids, the number of boxes will be

$$N_\varepsilon = \sum_{i,j} \text{ceil}\left[\frac{k\, d_\varepsilon(i,j)}{\varepsilon}\right],$$

where k is the coefficient of z-coordinate modification expressed as $k = R/G$, and ceil(x) stands for the ceiling of x. The condition for determining the upper limit ε_{max} is

$$\text{ceil}\left[\frac{R}{\varepsilon_{max}}\right] + 1 \;\leq\; \text{ceil}\left[\frac{R}{(\varepsilon_{max} - 1)}\right]$$

while for the lower limit ε_{min} is

$$\varepsilon_{min} \;=\; R^{\frac{1}{3}}.$$

The fractal dimension $RDBC_d$ is given by the slope of the line that fits best the plot of $-\log(N_\varepsilon)$ against $\log(\varepsilon)$.

Morphological fractal (M)

Mathematical morphology as developed by Serra [24] is basically a set theory and it extracts the impact of a particular shape on an image by means of the concept of a structuring element (SE), which encodes primitive shape information. The transformed image is a function of the SE distribution in the original image. In particular, dilation of a set with an SE Y is given by the expression

$$X \oplus Y = \{x : Y^x \cap X \neq \phi\}$$

and erosion of a set X with an SE Y is given by

$$X \,\Theta\, Y = \{x : Y^x \subset X\},$$

where Y^x indicates the translation of a set Y with X.

The version of morphological fractal analysis proposed by Hu et al. [25] uses the rhombus element Y as the basic SE to perform a series of erosions and dilations whose scales are from $\varepsilon = 1$ to $\varepsilon = 7$, and the areas of these SE are 5, 13, 25, 41, 61, 85, and 113 pixels, respectively. The surface area at each scale ε can be calculated as follows

$$S(X, Y, \varepsilon) = \frac{\sum_{x,y \in M} \left(f_\varepsilon^u(x,y) - f_\varepsilon^l(x,y)\right)}{2\varepsilon},$$

where $f_\varepsilon^u(x,y)$ and $f_\varepsilon^l(x,y)$ indicate the ε-th dilation and the ε-th erosion, respectively. The morphological fractal dimension, M_d, is estimated from the slope (m) of the line that fits the plot $\log S(X,Y,\varepsilon)$ versus $\log \varepsilon$

$$M_d = 2 + m.$$

Mass fractal method (MF)

The mass fractal dimension, MF_d, is used to describe the heterogeneity and space-filling ability of an object. Anderson et al. [26] indicated that objects regarded as mass fractals are those that are porous and do not have a uniform internal mass distribution. MF_d is measured by filling the pore space of a binary image with progressively larger boxes, or pore m-pixels. The size of m begins at 1 and increases to maximum pore pixel size. The number of pore m-pixels or boxes that fit in the pore space is counted. As m increases, the number of boxes that fit within the pore space decreases. The MF_d value is estimated from the negative of the slope of the plot log (number of pore m-pixels) versus log m.

Spectral dimension or random walks method (RW)

Anderson et al. [26] showed that more than one fractal dimension needed to be measured for the complete characterisation of soil structure. They showed that the spectral dimension (RW_d) was a useful way of discriminating between structures with similar values of MF_d. For estimating RW_d, the method used by Crawford et al. [27] was used here, with the difference that the random walks were conducted through the cell wall space or background of the binarised bread-crumb images. For each walk, a starting pixel is randomly picked and then a random step is taken from the current pixel to a pixel that is eight-connected to the current pixel. This is repeated and if the new pixel has not been visited, then 1 is added to the number of distinct sites visited (S_n). If a step is taken into a site that has been visited previously (null step) then 1 is added to the number of steps taken and 0 is added to S_n. The individual walks were set to stop after 100 null steps, and the number of walks used was 1,000. The spectral dimension is calculated from a plot of $\log(S_n)$ versus log(number of steps taken, n). The slope of this line is $RW_d/2$. The algorithm computes RW_d for each individual walk and reports the mean value of RW_d for the 1,000 walks.

Statistical analysis

Using SAS v.8.2 (SAS Institute Inc, NC, USA), regression analyses ($\alpha = 0.05$) were performed between the bread crumb features (mean cell area, standard deviation of cell area and void fraction) and the fractal dimensions obtained from the six methods used.

Results and discussion

Four typical bread crumb images of different grain and porosity are shown in Fig. 1. Sample A is an example of a non-uniform open grain structure. Samples B and D show homogeneous textures with sample D being slightly finer than sample B. Sample C is an illustration of a coarse-to-fine texture with a combination of variously-sized cells. Figures 2, 3, 4, 5, 6 and 7 show the plots used to estimate the FD of the four samples with the six different techniques. This analysis was repeated for the 500 images. The logarithmic plot between the average absolute difference in pixel intensity (E) and pixel distance (d) is shown in Fig. 2. The Hurst coefficients H (and consequently the fractal dimensions) were determined from the slopes of the fitted lines for the individual bread crumb samples. The FBM method yielded a low Hurst coefficient for regions with little variation in grey level intensity across distances because the values of E were similar for various pixel distances (d). On the contrary, regions with large variations in intensity across distances showed larger values of E for larger d. A fine image (sample D) presented little variation in intensity across distances and so had a low Hurst coefficient and a higher FBM_d (2.509 in Table 1) while a coarsely-textured image (sample A) showed a higher variation in intensity for higher distances and thus a lower FBM_d (2.469).

Figure 3 illustrates the logarithmic plot between the averaged energy of the horizontal and vertical directions (E) against the frequencies (f) for the Fourier transform method. It can be seen that for low frequencies of the power spectrum, the variation in energy between samples was higher than it was at higher frequencies. Coarse-textured images (samples A and C) produced higher values of energy at low frequencies. On the contrary, fine-textured images, such as sample B and D, yielded lower energy values at low frequencies, and consequently a higher FFT_d (2.623 and 2.657, respectively, in Table 1). In Fig. 3, it can be noticed that the scale in which fractality can be observed spans about one decade (log frequency from 1 to 2). In general, upper and lower cut-offs are unavoidable when extracting fractal dimensions from real physical objects. While the lower cut-off is determined by the spatial resolution of the image, the upper cut-off is at most of the order of the system size. Often the fractal behaviour observable at small scales (higher frequencies) disappears at larger ones (low frequencies), providing evidence for the transition from heterogeneity to homogeneity

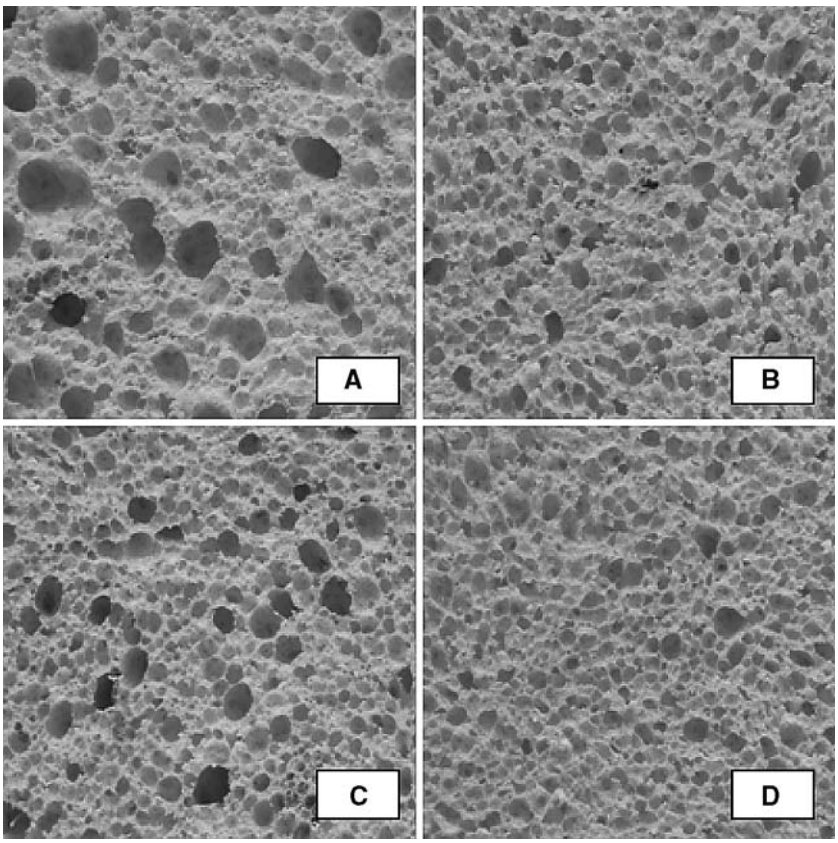

Fig. 1 Four bread crumb samples showing different grain and porosity characteristics. The void fractions calculated for the binary images of A, B, C and D were 0.502, 0.477, 0.494 and 0.469, respectively

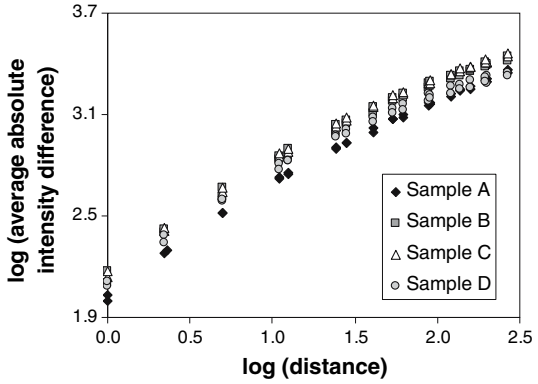

Fig. 2 Logarithmic plot of pixel distance versus average absolute difference in pixel intensity for the fractional Brownian motion method

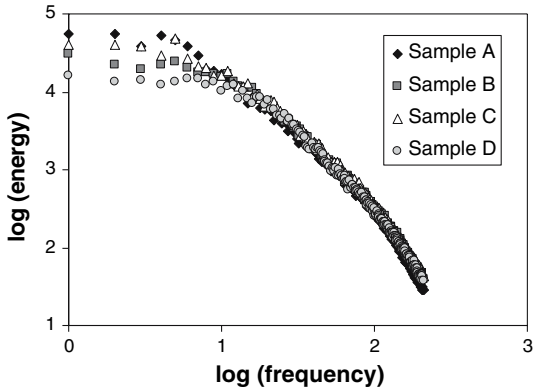

Fig. 3 Logarithmic plot of frequency versus averaged energy of the horizontal and vertical directions for the Fourier transform method

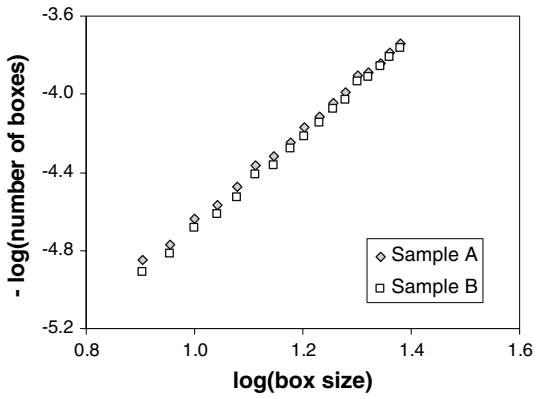

Fig. 4 Logarithmic plot of box size versus number of boxes for the relative differential box-counting method

Figure 4 is the logarithmic plot of box size (ε) versus the number of boxes (N_ε) that fit below the grey level intensity surface of the image. For clarity, samples C and D are not included. For smooth-textured images

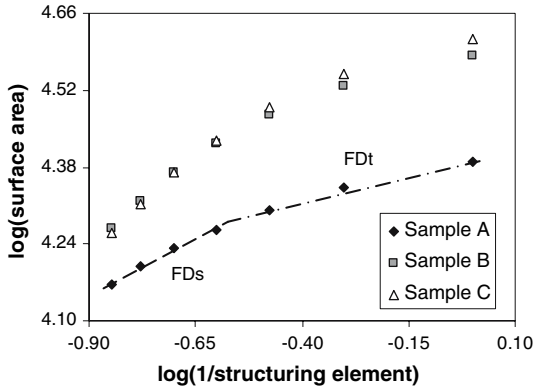

Fig. 5 Logarithmic plot of the inverse of the structuring element size versus pore-background surface area for the morphological method. All samples showed a structural fractal dimension (*FDs*) and a textural fractal dimension (*FDt*)

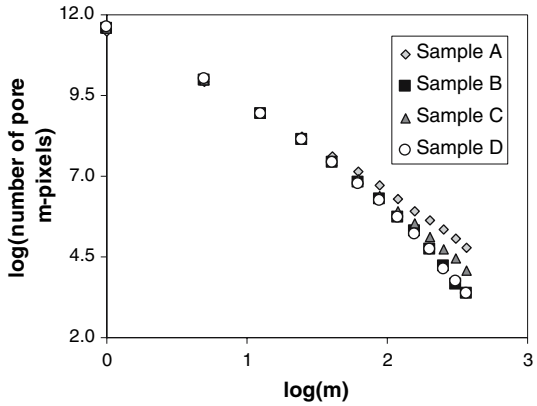

Fig. 6 Logarithmic plot of the box size (*m*) versus the number of boxes or pore *m*-pixels that fit into the image porous space for the mass fractal method

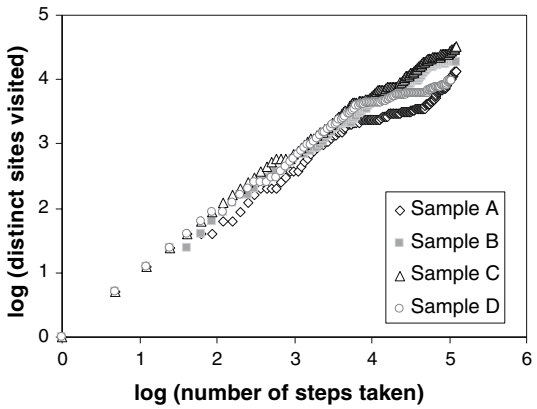

Fig. 7 Logarithmic plot of the number of steps taken against the distinct sites visited by one random walk through the non-porous space for the spectral method

Table 1 Fractal dimension values and coefficients of correlation of the samples found by the fractional Brownian motion method (FBM), the frequency domain method (FFT), the relative differential box-counting method (RDBC), the morphological method (M), the mass fractal method (MF) and the random walks method (RW) for the four typical bread crumb samples of Fig. 1

Sample	Fractal method					
	FBM	FFT	RDBC	M	MF	RW
A	2.469 (0.993)	2.552 (0.973)	2.372 (0.999)	2.261 (0.980)	2.326 (0.998)	1.685 (0.982)
B	2.487 (0.989)	2.623 (0.962)	2.446 (0.999)	2.368 (0.965)	2.938 (0.988)	1.669 (0.995)
C	2.484 (0.991)	2.608 (0.970)	2.445 (0.999)	2.415 (0.969)	2.656 (0.995)	1.674 (0.996)
D	2.509 (0.987)	2.657 (0.952)	2.447 (0.999)	2.375 (0.965)	2.962 (0.989)	1.649 (0.971)

with little variation in intensity (coarse crumb images), N_ε increased as ε increased, and $RDBC_d$ was smaller and close to the value 2.0. For rough-textured images with large variation in intensity (fine crumb images), the increment of N_ε was less than the increment in ε. Therefore, $RDBC_d$ was larger and close to 3.0. Because the $RDBC_d$ range turned out to be very limited for bread crumb samples (2.37–2.45), the plots for samples A and B were similar. The results in Table 1 for the four sample images, showed that the higher the $RDBC_d$ the finer the image.

Figure 5 presents the morphological estimation of M_d where the surface area between pores and background is logarithmically plotted against the inverse of the structuring element size. In this plot, sample A is positioned far from sample B and C due to its higher porosity. On the contrary, samples B and C were overlapped in the first four structuring elements. There is evidence [26, 28, 29] that some fractal objects may have two embedded surface fractal dimensions: structural (FDs) and textural (FDt). The structural fractal is typical of the overall structure of the surface and is the larger of the two, as the overall structure appears more rugged or irregular at low resolution. At high resolutions, instead, the FD becomes smaller indicating that the boundary is becoming more Euclidean (less rugged) and is referred to as textural fractal. Therefore, samples B and C may have similar structural fractal values but different textural ones. The presence of two embedded fractal dimensions in the bread crumb images was the general tendency and this indicates the susceptibility of the fractal dimension of crumb images to the scale or resolution at which it is evaluated. However, the morphological fractal dimensions shown in Table 1 were estimated from the slope of a single fitted straight line. For clarity, sample D was not shown in Fig. 5, as it greatly overlapped the data points of sample B.

Figure 6 is the logarithmic plot between box size and number of boxes to determine the pore mass fractal dimension of the samples which involve filling the binarised pore space with different box sizes. If the crumb grain image is predominantly formed of small discrete pores, only small boxes will fit in the pore space rather than large boxes. Because sample A presented large pores, a higher number of large boxes (high values of m in Fig. 6) fitted into the pore space and the mass fractal dimension was lower (lower slope). However, one sample may have a greater porosity than another (Fig. 1), but if the pore space is more heterogeneous, it will tend to have a smaller value of MF_d. This can be demonstrated with samples B and C. Ignoring the very few large cells of sample C (Fig. 1), samples B and C would present similar degree of coarseness. This is suggested by the RDBC method (fractal dimensions 2.446 and 2.445 in Table 1) and FBM (2.487 and 2.484) for samples B and C, respectively. Nevertheless, what makes sample B and C different is the degree of variation of cell size (heterogeneity of the texture). This difference is particularly shown by the mass fractal method (2.938 and 2.656). The MF_d values shown in Table 1 agree with what would be suggested from visual appraisal of grain homogeneity. Samples B and D presented approximately the same degree of grain homogeneity, and so their fractal dimensions were similar (2.938 and 2.962). Usually, a close grain was found very likely to exhibit a homogeneous texture and, conversely, an open grain to show a heterogeneous texture. However, even though they exhibit a close interrelation, fineness and homogeneity are better evaluated as separate characteristics. In this sense, Anderson et al. [26] found that their binary soil images were better described with three FD values instead of one.

Figure 7 shows the logarithmic plot between the number of steps taken and the distinct sites visited in one random walk for determining the spectral dimension (RW_d) of the samples. This value is related to the tortuosity of the cell wall space of the binarised image, which can be conceptually related to the uniformity of spatial distribution of the pores. The results shown in Table 1 and the coefficient of correlation between

MCA and RW_d (0.601 in Table 3) would suggest that an image with a high tortuosity of cell wall space (lower RW_d) will tend to have a finer texture. Thus, sample A, which showed the coarsest crumb, presented the highest RW_d (1.685 in Table 1). The spectral dimension was included here because it has demonstrated to contain information about the pore size and arrangement and to be a good discriminator of different pore structures in soil [26, 27].

The high coefficients of correlation for all methods to compute FD indicated the suitability of the macroscopic bread crumb structure to be adjusted to a surface fractal model. Based on the results from the 500 bread crumb images analysed, the highest R values corresponded to the RDBC method (0.998–0.999) and the MF method (0.982–0.999), followed by FBM (0.963–0.995), RW (0.961–0.998), M (0.944–0.999) and FFT (0.924–0.988) methods. The FD ranges were variable according to the method. The pore mass fractal and the morphological methods presented the highest ranges of fractal dimension: [2.087, 2.954] and [2.139, 2.626]. The ranges for the fractional Brownian motion, frequency domain, relative differential box-counting and random walks methods were [2.442, 2.589], [2.552, 2.742], [2.356, 2.541] and [1.599, 1.735], respectively. Likewise, the standard deviation values of the fractal dimensions computed by the methods were different (Table 2). Because the fractal dimension values depend on the fractal method used and on the type of images, the sensitivity of the fractal dimension to determine small changes in image texture may vary according to the method. In this way, Quevedo et al. [10] found, for their images of blooming chocolate (fat crystallisation), that the Fourier transform method was able to detect the blooming starting point while the box-counting method and the fractional Brownian motion method were insensitive.

The mean fractal dimension of bread crumb estimated using the relative differential box-counting method (2.438 ± 0.030) agreed closely with the average fractal dimension of cell wall of a hydrated starch foam (2.410 ± 0.16) estimated using a similar method [13]. This fractal dimension (2.438 ± 0.030) and the one derived using the fractional Brownian motion method (2.502 ± 0.024) were close to (1) the value of 2.544 obtained from scanning laser microscope surface height measurements of white bread slices [30] (in other words, very different techniques could give comparable values of the same structural feature), and to (2) the fractal dimension of 2.530 ± 0.02 of a 3-D randomly-branched network [31], implying that bread crumb has the structural characteristics of a sponge. These similarities would confirm that the visual appearance of bread crumb can be characterised by fractal analysis; and that, therefore, bread crumb's structure is likely to be self-similar over a limited range of magnification.

The inverse relationship between MCA and FD for the FBM, FFT, RDBC and MF methods indicated that the coarser the bread crumb grain, the lower the fractal dimension (Table 3). The MF method was the only method whose coefficient of correlation with stCA was higher than its coefficient of correlation with MCA. This fact would confirm what was previously suggested, that the MF method quantifies the heterogeneity of bread crumb grain. The M method and the RW method exhibited a positive relationship with MCA and stCA although their coefficients of correlation were the lowest. This is due to the fact that M_d and RW_d measure properties different than coarseness. While M_d quantifies the roughness on the interface cell–cell wall, RW_d measures the tortuosity of the cell wall phase and the pores distribution or arrangement. The results shown in Table 3 also suggest that for similar values of porosity (void fraction), the fractal dimension separated the different pore structures. The MF_d was the only fractal dimension whose regression with VF was not statistically significant. In contrast, the other fractal dimensions displayed a significant degree

Table 2 Mean and standard deviation of fractal dimensions of 500 bread crumb digital images

Fractal method	Mean	Standard deviation
Fractional Brownian motion (FBM)	2.502	0.024
Fast Fourier transform (FFT)	2.633	0.028
Relative differential box-counting (RDBC)	2.438	0.030
Morphological (M)	2.282	0.076
Mass fractal (MF)	2.661	0.194
Random walks (RW)	1.673	0.028

Table 3 Coefficients of correlation of the regressions between mean cell area (MCA), standard deviation of cell area (stCA) and void fraction (VF) with the fractal dimensions estimated from the different methods for the 500 bread crumb images analysed

Fractal method	R values		
	MCA	stCA	VF
Fractional Brownian motion (FBM)	–0.834	–0.572	0.296
Fast Fourier transform (FFT)	–0.802	–0.706	0.312
Relative differential box-counting (RDBC)	–0.786	–0.776	0.309
Morphological (M)	0.442	0.310	–0.482
Mass fractal (MF)	–0.714	–0.826	0.148[a]
Random walks (RW)	0.601	0.481	–0.518

[a] Analysis of variance was not significant

of correlation with void fraction ($P < 0.01$) although their coefficients of correlation were rather low (0.296–0.518). In other words, the porosity measurement or void fraction is not a property that can be used by itself to characterise pore structure because even though one sample may have the same void fraction as another, its pore space may be more heterogeneous or differently distributed spatially than the other. The fractal dimension allows for better quantification of these properties.

Conclusions

The visual appearance of bread crumb can be successfully characterised by the fractal dimensions of its digital image. Due to its morphological irregularities, the bread crumb macroscopical structure can be approached as one of an apparent fractal object. Even though the fractal dimension ranges varied according to the method used, they were able to accurately describe the roughness of the intensity surfaces of bread crumb images. The fractal dimensions obtained from the fractional Brownian motion method and the relative differential box-counting method measured bread crumb coarseness. The higher the fractal dimension, the finer the bread crumb appearance. Evidence indicates that the mass fractal dimension quantified better the crumb heterogeneity rather than the crumb coarseness. The fractal dimensions from the morphological method and the random walks method showed the lowest coefficients of correlation with mean cell area and standard deviation of cell area. The basis of their method of calculation suggests that the morphological fractal measures the jaggedness on the interface cell–cell wall, and that the random walks method quantifies the tortuosity of the cell wall and pores arrangement. Although the fast Fourier transform method adjusted bread crumb images to a fractal model with the lowest coefficient of correlation of all methods ($R = 0.924$–0.988), its fractal dimension was still related to bread crumb coarseness. The low correlation between fractal dimension and void fraction ($R = 0.296$–0.518) indicated that the latter feature should not be used by itself to parameterise the bread crumb structure as even two samples having similar porosity, might present a different degree of cell heterogeneity or distribution. Fractal analysis should be applied for a better description of bread crumb appearance by the use of a vector containing several fractal dimensions.

Acknowledgments This work was funded by the Irish Department of Agriculture through the Food Institutional Research Measure. The Authors wish to acknowledge Dr. Roberto Quevedo León from the Department of Food Science and Technology, Universidad de Los Lagos, Chile, for his assistance with the mass fractal method and the random walks method.

References

1. Kamman PW (1970) Bakers' Dig 44(2):34–38
2. Pyler EJ (1988) Baking science and technology, vol 2, 3rd edn. Sosland Publishing Company, Kansas
3. Weixing Z, Tiejun Z, Tao W, Zunhong Y (2000) Chem Eng J 78:193–197
4. Lencki RW, Riedl K (1999) Food Res Int 32:279–288
5. Norton RT, Mitchell JR, Blanshard MV (1998) J Tex Stud 29:239–253
6. Barret AH, Peleg M (1995) Lebensm-Wiss Technol 28:553–563
7. Peleg M, Normand M (1985) J Food Sci 50:829–831
8. Dziuba J, Babuchowskii A, Smoczynski M, Smietana Z (1999) Int Dairy J 9:287–292
9. Hagiwara T, Wang H, Suzuki T, Takai R (2002) J Agric Food Chem 50:3085–3089
10. Quevedo R, López C, Aguilera J, Cadoche L (2002) J Food Eng 53:361–371
11. Amaku M, Moralles M, Horodynski-Matsushigue LB, Pascholati PR (2001) Revista Brasileira de Ensino de Física 23(4):422–428
12. Narine SS, Marangoni AG (1999) Phys Rev E 59(2B):1908–1920
13. Liu Z, Chuah CSL, Scanlon MG (2003) Act Materialia 51:365–371
14. Mandelbrot BB (1983) The fractal geometry of nature. W. H. Freeman, San Francisco
15. Pentland A (1984) IEEE Trans PAMI 6:661–674
16. Gonzales-Barron U, Butler F (2006) J Food Eng 74:268–278
17. Huang LK, Wang MJ (1995) Pattern Recognit 21(1):41–51
18. Chan KL (1995) IEEE Trans Biomed Eng 42(10):1033–1037
19. Russ JC (2002) Handbook of image processing, 4th edn. CRC Press, Boca Raton
20. Buczkowski S, Kyriacos S, Nekka F, Cartilier L (1998) Pattern Recognit 31(4):411–418
21. Biswas MK, Ghose T, Guha S, Biswas PK (1998) Pattern Recognit Lett 19:309–313
22. Bisoi AK, Mishra J (2001) Pattern Recognit Lett 22:631–637
23. Jin XC, Ong SH, Jayasoriah (1995) Pattern Recognit Lett 16:457–464
24. Serra J (1982) Image analysis and mathematical morphology, vol 1. Academic, New York
25. Hu J, Xin B, Yan H (2002) Textile Res J 72(10):879–884
26. Anderson A, McBraney A, Fitzpatrick E (1996) Soil Sci Soc Am J 60:962–969
27. Crawford JW, Ritz K, Young IM (1993) Geoderma 56:157–172
28. Peleg M (1993) Crit Rev Food Sci Nutr 33(2):149–165
29. Kaye BH (1995) Chaos Solitons Fractals 6:245–253
30. Pedreschi F, Aguilera JM, Brown CA (2000) J Food Process Eng 23(2):127–143
31. Jan N, Stauffer D (1998) Int J Mod Phys C 9(2):341–347